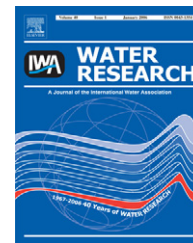


Available at [www.sciencedirect.com](http://www.sciencedirect.com)journal homepage: [www.elsevier.com/locate/watres](http://www.elsevier.com/locate/watres)

# An autopsy study of a fouled reverse osmosis membrane element used in a brackish water treatment plant

Thuy Tran<sup>a,\*</sup>, Brian Bolto<sup>a,\*</sup>, Stephen Gray<sup>b,\*</sup>, Manh Hoang<sup>a</sup>, Eddy Ostarcevic<sup>c</sup>

<sup>a</sup>CSIRO Manufacturing & Materials Technology, Private Bag 33, Clayton South, Vic. 3169, Australia

<sup>b</sup>Victoria University, Werribee Campus, PO Box 14428, Melbourne, Vic. 8001, Australia

<sup>c</sup>GWMWater, PO Box 481, Horsham, Vic. 3402, Australia

## ARTICLE INFO

### Article history:

Received 14 February 2007

Received in revised form

5 June 2007

Accepted 7 June 2007

Available online 12 June 2007

### Keywords:

Reverse osmosis

Fouling

Water treatment

Desalination

Fouling mechanisms

## ABSTRACT

The fouling of a spiral wound reverse osmosis (RO) membrane after nearly 1 year of service in a brackish water treatment plant was investigated using optical and electron microscopic methods, Fourier transform infrared spectroscopy (FTIR) and inductively coupled plasma atomic emission spectrometry (ICP-AES). Both the top surface and the cross-section of the fouled membrane were analysed to monitor the development of the fouling layer. It has been found that the extent of fouling was uneven across the membrane surface with regions underneath or in the vicinity of the strands of the feed spacer being more severely affected. Fouling appeared to have developed through different stages. In particular, it consisted of an initial thin fouling layer of an amorphous matrix with embedded particulate matter. The amorphous matrix comprised organic–Al–P complexes and the particulate matter was mostly aluminium silicates. Subsequently, as the fouling layer reached a thickness of about 5–7  $\mu\text{m}$ , further amorphous material, which is suggested to include extracellular polymeric substances such as polysaccharides, started to deposit on top of the existing fouling layer. This secondary amorphous material did not seem to contain any particulate matter nor any inorganic elements within it, but acted as a substrate upon which aluminium silicate crystals grew exclusively in the absence of other foulants, including natural organic matter (NOM).

Crown Copyright © 2007 Published by Elsevier Ltd. All rights reserved.

## 1. Introduction

Reverse osmosis (RO) is a commonly used process in desalination and advanced wastewater treatment. However, like other membrane filtration processes, fouling is a major obstacle in the efficient operation of RO systems. Membrane fouling causes deterioration of both the quantity and quality of treated water, and consequently results in higher treatment costs. Foulants may be classed into one of four major categories: sparingly soluble inorganic compounds, colloidal or particulate matter, dissolved organic substances and microorganisms (Speth et al., 2000). Fouling by sparingly

soluble inorganic compounds is governed by concentration polarization and scale layer formation when the product of the concentration of the soluble components exceeds the solubility limit (Boerlage et al., 1999). Particulate and colloidal matter rejected by the membrane may form compact cakes, which introduce an additional resistance barrier to filtration (Gabelich et al., 2002). Organic fouling is governed in part by interactions between the membrane surface and the organic foulants, as well as between the organic foulants themselves (Dalvi et al., 2000). Microbial attachment and growth on the membrane surface leads to the formation of biofilms, which consist of microbial cells embedded in an extracellular

\*Corresponding authors. Tel.: +61 3 9545 2046; fax: +61 3 9544 1128.

E-mail addresses: [thuy.tran@csiro.au](mailto:thuy.tran@csiro.au) (T. Tran), [brian.bolto@csiro.au](mailto:brian.bolto@csiro.au) (B. Bolto), [stephen.gray@vu.edu.au](mailto:stephen.gray@vu.edu.au) (S. Gray).  
0043-1354/\$ - see front matter Crown Copyright © 2007 Published by Elsevier Ltd. All rights reserved.  
doi:10.1016/j.watres.2007.06.008

polymeric substances matrix produced by the microbes (Ivnitskya et al., 2005). Despite various research efforts, to date the characterization of seawater fouling of RO membranes has not progressed significantly, compared with low-pressure membrane fouling by surface and ground waters (Kumar et al., 2006).

Although membrane fouling is traditionally measured by flux decline with time, this method is inadequate for characterizing fouling development in a RO process. It has been shown that when the permeate flux is noticeably affected, the membrane is so severely fouled that restoration to its original permeability may become impossible (Tay and Song, 2005). Autopsies of fouled membranes have also been carried out in order to better understand the physico-chemical processes governing the fouling (see, for example, Butt et al., 1997; Speth et al., 1998; Sahachaiyunta et al., 2002; Vrouwenvelder and van der Kooij, 2002; Gwona et al., 2003). The methods of chemical and structural analyses used in these studies including inductively coupled plasma mass spectrometry (ICP-MS), gas chromatography/mass spectrometry (GC-MS), Fourier transform infrared spectroscopy (FTIR) and X-ray diffraction (XRD) provide only the average composition of the surface deposits. Because these deposits are complex and heterogeneous, information on average composition is of limited value in elucidating the fouling mechanisms. Direct observations using optical and electron microscopic methods, including scanning electron microscopy (SEM) and associated energy-dispersive X-ray spectroscopy (EDS), often focus on the top surface deposits, but not on the underlying deposit layers. This leads to an incomplete understanding of the deposition kinetics of various foulants, and therefore of the fouling mechanisms, particularly where thicker deposits have been developed.

Another issue is that while the distinction between inorganic, colloidal, organic, and biological fouling is useful, RO membranes in a typical operation are likely to be exposed to all categories of foulants. Because of the complex nature of fouling, many mechanistic studies on RO membrane fouling have focused on one foulant type for the purpose of simplicity. However, it is very important to understand the effects of interactions between various foulant types on the fouling mechanisms. For instance, it has recently been reported that the enhanced concentration polarization of salt ions within the colloidal cake layer may result in an increase in osmotic pressure and rapid flux decline during cake layer development (Hoek and Elimelech, 2003; Lee et al., 2005). Also, interactions between colloidal and organic foulants have been found to give rise to considerable synergistic effects, as manifested by a significantly higher flux decline compared with the additive effects of colloidal fouling and organic fouling alone (Li and Elimelech, 2006).

This paper presents the autopsy results of a spiral wound RO membrane after nearly 1 year of service in a water treatment facility. Analytical techniques used in the investigation of the surface deposits include inductively coupled plasma atomic emission spectrometry (ICP-AES), FTIR, optical and electron microscopic methods. Both the top surface and the cross-section of the fouled membrane were analysed to provide further insights into the development of the fouling layer.

## 2. Materials and methods

### 2.1. The fouled spiral wound RO membrane element

The fouled RO membrane element (FILMTECH, BW30LE-440DRY) selected for the autopsy study had been in service for nearly 1 year in a water treatment facility operated by GWMWater in Hopetoun, western Victoria, Australia. The RO desalination plant was integrated into the water treatment facility in response to the increased salinity of surface water in the region due to the extended drought in recent years. The plant was capable of producing 250 KL/d of permeate and included a concentrate recycle stream to improve recovery to 80%. A phosphonate-based antiscalant was used in the RO operation and pre-chlorination was not carried out in the treatment process because of the high levels of disinfection by-product precursors.

Prior to the RO treatment, the raw water from catchments in the Grampians Ranges and stored in open reservoirs had undergone a pre-treatment process including coagulation (aluminium sulphate), flocculation, dissolved air flotation and filtration (DAFF), pH correction, and cartridge filtration using 5 and 1 µm pore size filters. The filtered water had a pH of 9.1, a total dissolved solids of 900 mg/L, a total organic carbon of 12 mg/L and a turbidity of 0.5 NTU. Chemical analysis of the filtered water was carried out and the results are presented in Table 1.

The extended drought created conditions that promoted algal growth in the storage reservoirs and this change had a detrimental effect on the performance of the DAFF process as well as on the desalination plant, resulting in a significant decline in production. The algal outbreak required clean-in-place events to be scheduled every month, but the flux

**Table 1 – Results of chemical analysis of filtered water prior to RO treatment process**

Elements <sup>a</sup>	Concentration (mg/L)
Bicarbonate, HCO <sub>3</sub> <sup>-</sup>	59
Carbonate, CO <sub>3</sub> <sup>2-</sup>	<1
Ba	0.099
Ca	29
Cl	410
Fe	<0.02
K	6.1
Mg	31
Mn	0.004
N, nitrate	0.006
Na	180
P	0.007
S	25
Si, total as SiO <sub>2</sub>	3.3
Sr	0.33

<sup>a</sup> The analysis was carried out using either ICP or ICP/MS. Chloride and nitrogen concentrations were determined using potentiometric titration and colorimetric methods, respectively. Bicarbonate level was determined using bicarbonate titration with electrometric endpoint.

decline was significant and the original aim of operating at 80% recovery was not possible. Even after the DAFF process was optimized to remove the algal cells and better water was secured from another reservoir, the RO desalination plant could only operate at 75% recovery at best.

Following the algal outbreak, a fouled RO membrane element was selected for the autopsy study. Surface deposits were scraped from the fouled membrane surface and analysed by ICP-AES and FTIR. The middle section between the feed end and the concentrate end of the fouled membrane was also cut into various coupons and prepared for optical and electron microscopic studies.

## 2.2. ICP-AES analysis

Surface deposits were digested in duplicate with 1:1 HNO<sub>3</sub> on a hotplate prior to analysis by using a Varian Vista ICP-AES. A general scan including Al, As, Au, Ba, Be, Bi, Ca, Cd, Ce, Co, Cr, Cu, Fe, Ga, Ge, Hf, Hg, In, K, La, Mg, Mn, Mo, Na, Nb, Ni, P, Pb, Pd, Pt, S, Sb, Se, Si, Sn, Sr, Ta, Th, Ti, U, V, W, Y, Zn and Zr elements was carried out. Only the elements detected in trace levels and above are reported in the results. Chloride concentrations were determined by analysing the sample in duplicate by potentiometric titration with silver nitrate.

## 2.3. FTIR analysis

Approximately 1.5 mg of dried sample was ground and mixed with approximately 50 mg of anhydrous KBr and subsequently pressed into a disc. FTIR spectra (500–4000 cm<sup>-1</sup>) of the discs were obtained using a Perkin Elmer 2000 FT-IR spectrophotometer in transmission mode with KBr as the background reference.

## 2.4. Optical and electron microscopic analyses

An Olympus BHS Metallographic Optical Microscope was used for general observation of the fouled membrane sections. Microstructures of the surface deposits were analysed using a Philips XL30 field emission SEM operating at 5–15 kV in conjunction with EDS to obtain chemical information. EDS spot analysis using a spot diameter of about 3 nm at selected areas on the samples was carried out. Since the X-ray sampling volume is close to the electron-sample interaction volume, the spot analysis data typically included X-ray signals generated from a sampling volume of about 1 μm<sup>3</sup> (Goodhew and Humphreys, 1992).

Both the top surface and the cross-section of the fouled membrane coupons were analysed. For the top surface analyses, the membrane coupons were mounted on a holder using double-sided carbon tape. For the cross-section analyses, the coupons were embedded in a polymeric resin in such a way that their cross-section was oriented perpendicular to the incoming light/electron beam. The samples were then polished with various grades of diamond paste using oil-based lubricant before analyses.

# 3. Results and discussion

## 3.1. General observations by optical microscopy

Generally, the deposits were distributed unevenly across the membrane surface. Optical images of the membrane surface before and after the feed spacer was removed are shown in Figs. 1a and b, respectively. It can be seen that regions underneath or in the vicinity of the spacer strands were covered by brown stains, whereas the extent of staining in regions located further away was generally less severe and varied considerably. Examination of regions near the strands at higher magnifications also revealed the occasional presence of microorganisms, as shown in the inset of Fig. 1b.

Uneven fouling is also evident from the investigation of the cross-sections, which showed a considerable variation in the thickness of the surface deposits. In particular, many deposits in regions underneath or close to the spacer strands had a thickness of about 90 μm or more, as illustrated in Fig. 2(a), whereas those located further away were thinner and had a thickness ranging from less than 1 to about 25 μm, as shown in Figs. 2(b) and (c).

A major objective of using the feed spacer is to promote eddy mixing, which increases mass transfer and reduces concentration polarization (Belfort and Guter, 1972). While turbulence is created between spacer strands, it is also known that the spacer may promote excessive particle precipitation in regions close to the strands (Gimmelshtein and Semiat, 2005). This undesirable effect is evident in the present study from the observation of thick deposits in these regions. The presence of thick deposits could lead to detrimental consequences. In particular, they could act as an effective barrier to prevent water in the local environment from penetrating through the underlying membrane, and therefore could greatly diminish the local water flux. They could also have adverse effects on the feed flow properties, for instance, by distorting the flow path and lowering the cross-flow velocity in the feed channel, which could in turn contribute to the uneven and enhanced fouling across the membrane surface.

The difficulty in characterizing fouling is often attributed to the complexity of feed water composition and to the different fouling mechanisms of different foulant types. Feed water is usually characterized using common water analysis parameters such as the concentration of each foulant present in the water. The flow properties and rate of fouling are often assumed to be uniform throughout the membrane surface. The observations in the present study highlight the importance of local variations in the hydrodynamic conditions in that they may lead to considerable uneven fouling, and therefore should be featured more prominently in the characterization of RO membrane fouling.

## 3.2. Analyses of surface deposits by ICP-AES and FTIR

The results from ICP-AES analysis are shown in Table 2. Major elements detected included Al (2570 ppm), Ca (2760 ppm) and P (1225 ppm). Lesser amounts of Fe (590 ppm), S (865 ppm), Si (410 ppm), Mg (320 ppm), K (110 ppm) and Na (190 ppm) were also present. A relatively high level of Cl was detected



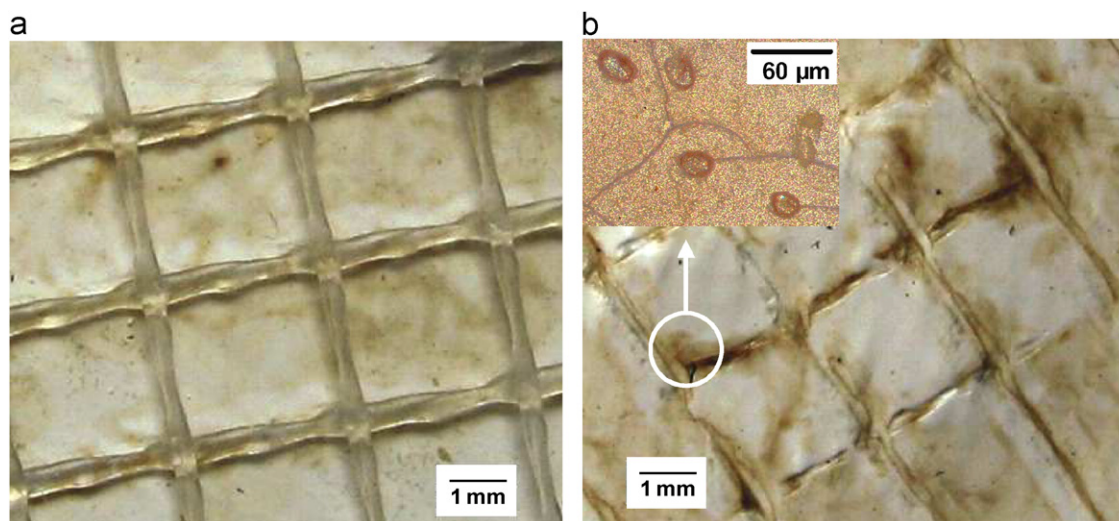


Fig. 1 – Optical images of the membrane surface before (a) and after (b) the feed spacer was removed.

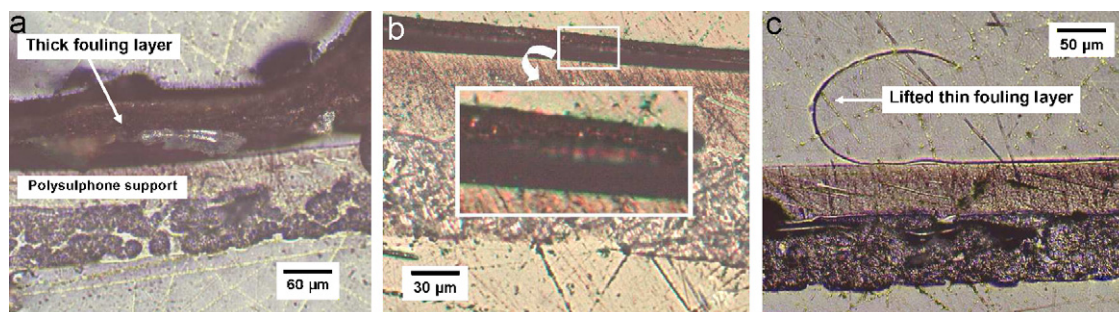


Fig. 2 – Optical images showing (a) a thick fouling layer in regions near the spacer strands and (b) and (c) a fouling layer with varying thickness in regions located further away from the strands.

Table 2 – Results of ICP-AES analyses of deposits scraped from the fouled membrane surface

Elements <sup>a</sup>	Concentration (mg/kg)
Ag	60
Al	2570
Ba	14
Ca	2760
Cl	1430
Cr	24
Cu	20
Fe	590
K	110
Mg	320
Na	190
Ni	22
P	1225
S	865
Si	410
Sr	23
Ti	5.4
Zn	35
Zr	19

<sup>a</sup> Chloride concentration was determined using potentiometric titration.

(1430 ppm). Low levels of Ba, Cr, Cu, Ni, Sr, Ti, Zn and Zr were also identified in the deposits.

Generally, the presence of negative ions, including bicarbonate, silicate and sulphate, in the RO feed is important for the precipitation of various compounds. Common deposits found on fouled RO membranes include aluminium silicates, carbonate compounds of Ca and Mg, and sulphate compounds of Ca, Sr and Ba (see, for example, [Yiantsios et al., 2005](#); [Butt et al., 1997](#)). Metal ions, most notably  $\text{Ca}^{2+}$ , may also form complexes with natural organic matter (NOM), giving rise to the subsequent formation of intermolecular bridges among organic foulant molecules and enhanced membrane fouling ([Li and Elimelech, 2004](#)). Also, where a fouling layer has developed on the membrane surface, the layer may entrap and hinder back-diffusion of dissolved salt ions, resulting in an increase in concentrations of salt ions near the membrane surface ([Herzberg and Elimelech, 2007](#); [Hoek and Elimelech, 2003](#)).

These deposition mechanisms could operate during the development of the fouling layer in the current case, resulting in various types of deposits detected on the fouled membrane surface. It is noted that the use of aluminium sulphate coagulant and phosphonate-based antiscalant prior to the RO treatment could also raise the levels of Al, S and P in the feed

and contribute to the relatively high levels of these elements in the deposits. This issue will be discussed further in a later section. Also, while only a trace amount of Fe was detected in the RO feed, a relatively high level of Fe was present on the fouled membrane deposits. A similar finding was also reported in a previous study by Gwona et al. (2003), who attributed the high residual Fe levels on the fouled membranes, even after all cleanings, to irreversible fouling.

A typical FTIR spectrum of the fouled membrane extract is shown in Fig. 3. The main absorption bands were in the vicinity of  $3428\text{ cm}^{-1}$  (O–H stretching and N–H stretching),  $2920\text{ cm}^{-1}$  (aliphatic C–H stretching),  $1631\text{ cm}^{-1}$  (C=O stretching of amide I, quinone and ketones),  $1563\text{ cm}^{-1}$  (N–H deformation+C–N stretching of amide II, symmetric stretching of COO<sup>−</sup>) and  $1078\text{ cm}^{-1}$  (C–O stretching of polysaccharides). The band in the vicinity of  $1400\text{ cm}^{-1}$  could be due to aliphatic C–H deformation, C–O stretching and O–H deformation of phenol. The band in the range  $600\text{--}800\text{ cm}^{-1}$  could be due to aromatic compounds. These results suggest that the constituents of the membrane fouling matter included

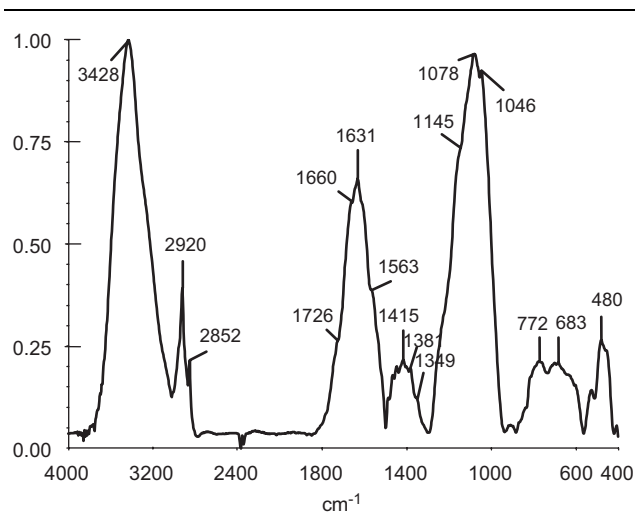


Fig. 3 – FTIR spectrum of the fouled membrane extract.

proteins, polysaccharides, and aliphatic and aromatic compounds derived from humic substances.

### 3.3. Investigation of the membrane surface and cross-sections by SEM/EDS

Generally, the SEM/EDS investigation confirms the variation in the extent of fouling across the membrane surface as observed by optical microscopy, and gives further insights into the development and nature of the fouling layer. As shown in Fig. 4, a typical fouled membrane surface consisted of particulate matter embedded in an apparently amorphous matrix. Associated EDS analyses indicate that the particulate matter had relatively high levels of C, O, Al and Si, whereas the matrix had high levels of C, O, Al and P. Quite low levels of Ca, Mg, Cl and S were also present. Scales containing high levels of Si and Al, as shown in Fig. 5, were often observed.

The C and O peaks are likely due in part to organic and/or biological materials. The high levels of Al and Si in the particulate matter suggest that it was mainly aluminium silicates, which are common foulants in RO operations. Given that cartridge filtration with 5 and  $1\mu\text{m}$  pore size filters had been used to pre-treat the water, the RO feed was likely to be free from larger size silt/clay particles. However, finer particles might remain in the feed and subsequently form part of the fouling layer. The use of aluminium sulphate as coagulant prior to the RO treatment could also elevate the Al concentration in the RO feed and contribute to the formation of aluminium silicates (Gabelich et al., 2005). It is noted that phosphonate-based antiscalants, as used in the present case, have been reported to be ineffective for suppressing the precipitation of aluminum silicates (Gabelich et al., 2005; Butt et al., 1995). The use of phosphonate-based antiscalant in the present case could also contribute to the relatively high levels of P observed in the matrix. It is possible that in the presence of metal ions such as  $\text{Al}^{3+}$  that act as cationic “anchors”, there would be strong interactions between anionic humates and phosphates (Riggle and von Wandruszka, 2005). A previous study has also suggested that phosphorus from

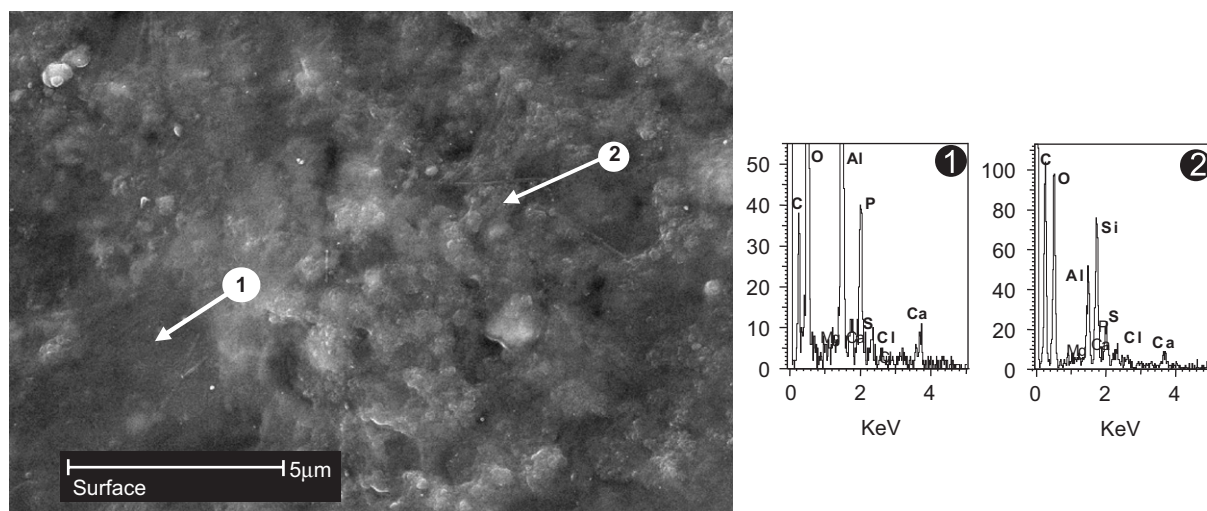


Fig. 4 – SEM micrograph and associated EDS showing particulate matter embedded in an amorphous matrix.

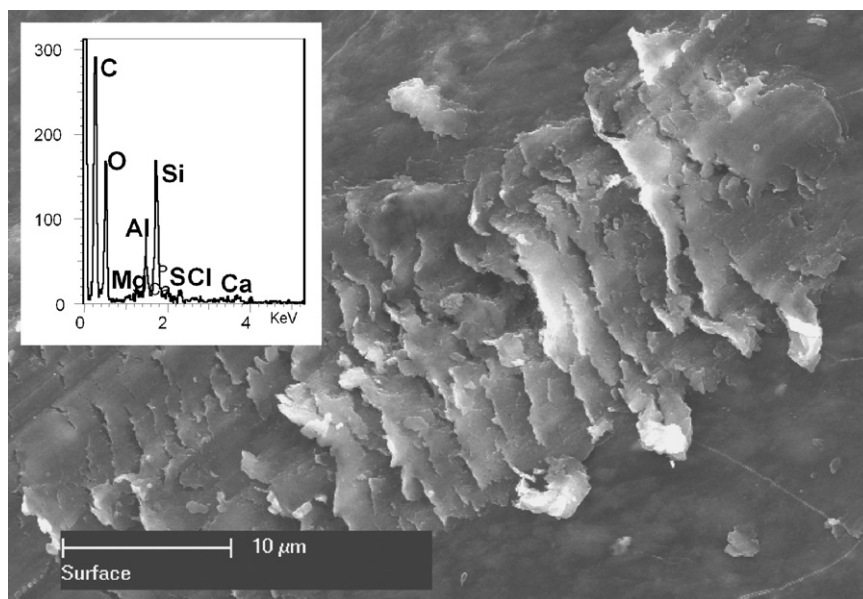


Fig. 5 – SEM micrograph and associated EDS showing aluminium silicate scaling.

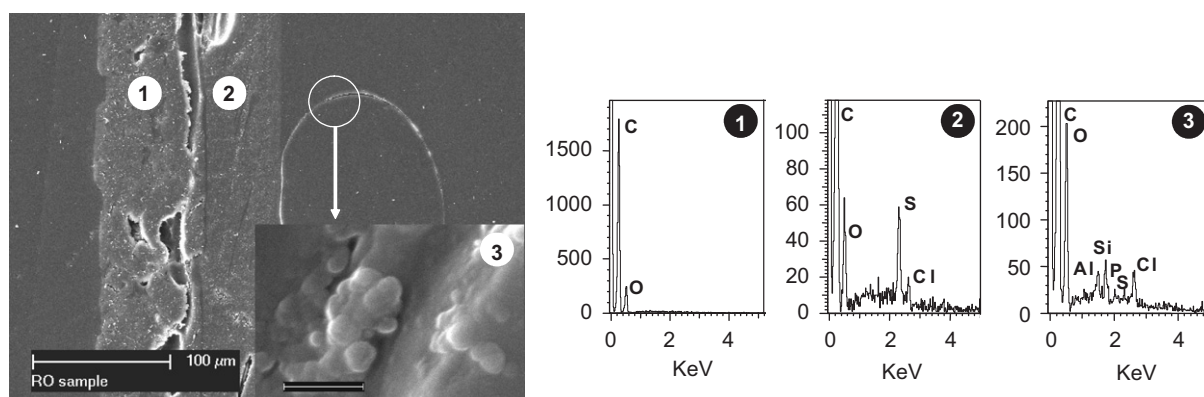


Fig. 6 – SEM micrographs showing a thin fouling layer at different magnifications and associated EDS analyses. Bar (inset) = 500 nm.

phosphonate-based antiscalants can react with aluminium to form precipitates on RO membrane surfaces (Gabelich et al., 2005). Another possibility is that calcium phosphate, which has a low solubility, could precipitate and form part of the matrix. However, given the relatively low levels of Ca compared with those of P, the possible presence of calcium phosphate in the matrix would not be a major factor contributing to the high levels of P in the matrix.

The SEM/EDS investigation of the cross-sections of the membrane gives further insights into the development of the fouling layer. Micrographs of a thin fouling layer at different magnifications and associated EDS analyses are shown in Fig. 6. Note the similarity between Fig. 6 and the optical image of the same section at similar magnification presented in Fig. 2c. EDS analysis of the microporous support layer showed S and Cl. The presence of S is likely due to polysulphone, whereas Cl ions could have diffused through the polyamide skin layer with some retained in the microporous support. In contrast, Cl was absent in the fabric layer. It is possible that

once Cl reached this layer, mass transport would be more efficient and most Cl would diffuse into the bulk of the permeate.

The fouling layer presented in Fig. 6 had a thickness of less than 1 µm and consisted of particulate matter embedded in an apparently amorphous matrix. These features are similar to those observed at the top surface of the fouled membrane. EDS analysis of this layer also showed the presence of Al, Si, P, S and Cl. As discussed above, aluminium silicates and the association of organic–Al–P could contribute to the Al, Si and P peaks, whereas the Cl peak is likely due to the entrapment of dissolved Cl ions in the fouling layer. Although it is possible that parts of the underlying polysulphone membrane could be lifted together with the fouling layer and thus contribute to the S peak, analyses of the thicker fouling layer, as will be shown below, suggest that sulphur is part of the fouling layer.

Similar features were also observed in the thicker fouling layer. A typical example is shown in Fig. 7 with associated EDS analyses. In this case, the fouling layer was about 3 µm thick



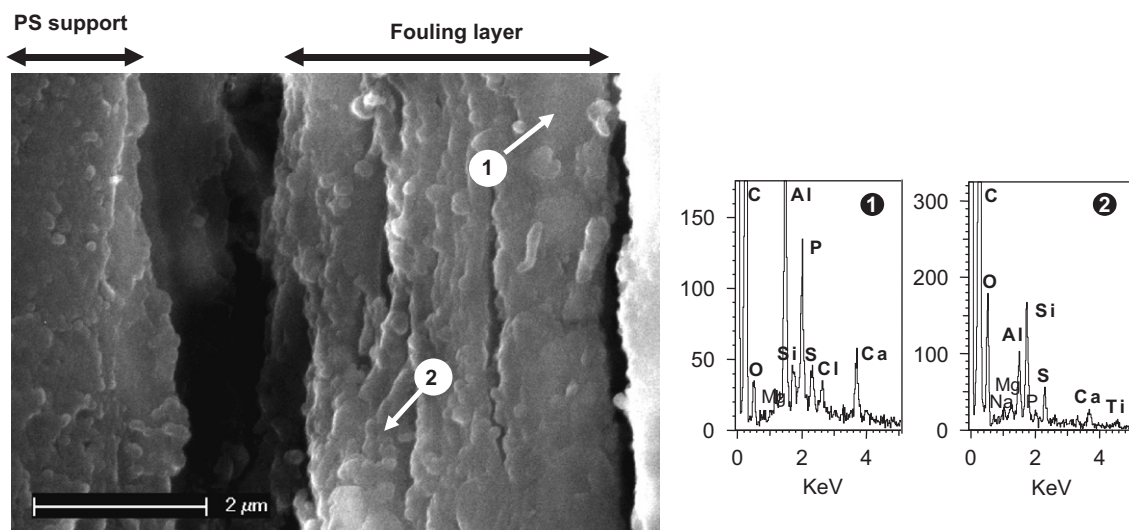


Fig. 7 – SEM micrograph and associated EDS analyses showing a thicker fouling layer.

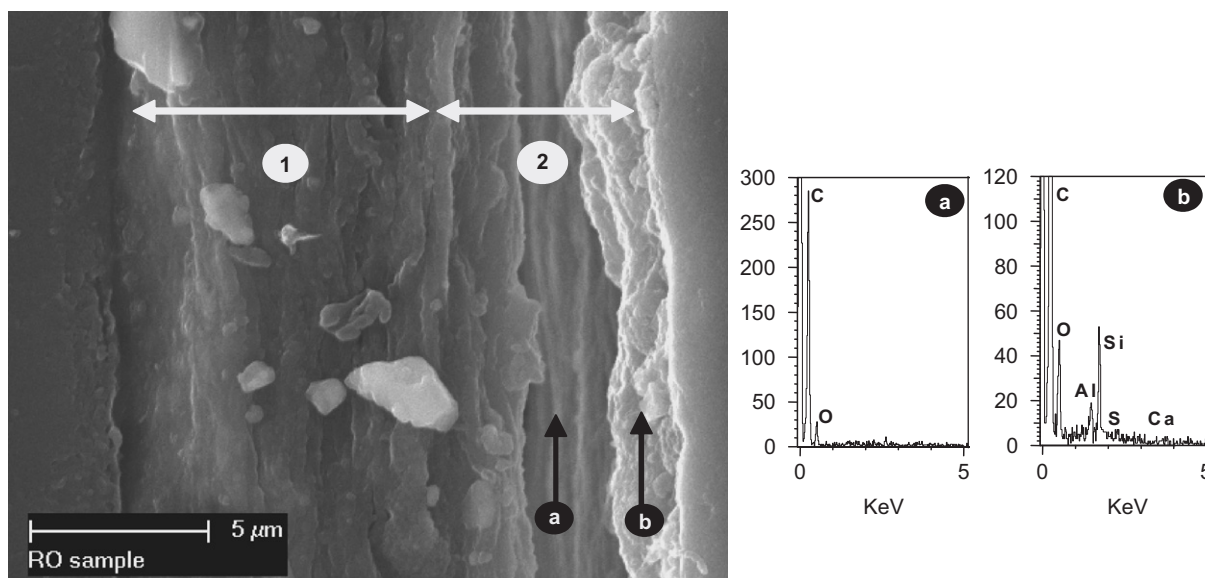


Fig. 8 – SEM micrograph showing two distinct regions (1 and 2) of a thick fouling layer and EDS analyses of the inner amorphous (a) and outer crystalline (b) layers of region 2.

and, similar to the case of a thinner fouling layer, consisted of an amorphous organic–Al–P matrix embedded with aluminium silicates. Sulphur was present in regions located away from the surface of the microporous support (area 1 in Fig. 7). A range of elements including Ca, Mg, Na, Fe, Cl and Ti were also present in lesser amounts.

For a fouling layer with a thickness greater than about 10 μm, additional features were observed. A typical micrograph and associated EDS analyses of such a layer are shown in Fig. 8. It can be seen that the layer consisted of two distinct regions. Region 1 had a thickness ranging from about 5 to 7 μm and was similar to the thinner fouling layer shown in Fig. 7 in that it had an amorphous organic–Al–P matrix with aluminium silicates embedded within (EDS analysis is not presented here).

Region 2 was structurally and chemically different from region 1 and had two distinct zones: an inner amorphous layer and an outer crystalline layer. It can be seen in Fig. 8 that the outer crystalline layer consisted of mainly aluminium silicate crystals. In contrast, there was no particulate matter embedded within the inner amorphous layer and the EDS analysis of this layer did not detect any elements except carbon and oxygen. NOM is unlikely to be a major constituent of this layer, given the tendency of NOM to incorporate inorganic matter within its matrix as is the case for region 1. One possibility is that this layer was proteinaceous in nature and included extracellular polymeric substances such as polysaccharides produced by microbes. This hypothesis is consistent with the detection of polysaccharides in the fouling layer by FTIR. Their late appearance in fouling

development may reflect the biofouling episodes due to the algal outbreak, which occurred at the later phase of RO operation. It is interesting that while there was neither particulate matter nor inorganic element associated with the inner amorphous layer, the layer acted as a substrate upon which aluminium silicate crystals grew exclusively in the absence of other foulants including NOM. It is noted that a variety of polysaccharides have been used to reduce biological fouling of surfaces due to their ability to provide steric barrier and electrostatic repulsion that hinder adsorption (Hartley et al., 2002). In the present case, these properties of polysaccharides could play a role in facilitating crystal growth, but had the effect of preventing the deposition of larger foulants.

#### 4. Conclusions

This paper presents the autopsy results of a spiral wound RO membrane after nearly 1 year of service in a brackish water treatment plant using optical and electron microscopic methods, FTIR and ICP-AES. Both the top surface and the cross-section of the fouled membrane were analysed to provide further insights into the development of the fouling layer. The results obtained from different techniques are consistent and complementary to each other. A number of conclusions are made:

1. The extent of fouling was uneven across the membrane surface with regions underneath or in the vicinity of the feed spacer strands being most affected. The fouling in regions located further away from the strands was generally less severe, but varied considerably. These results highlight the importance of local variations in the hydrodynamic conditions in characterizing RO fouling.
2. The major inorganic elements in the fouling layer included Al, Ca and P. The use of aluminium sulphate coagulant and phosphonate-based antiscalant could contribute to the high levels of Al and P. Lesser amounts of Fe, S, Si, Mg, K and Na were also present. Other constituents of the fouling layer included proteins, polysaccharides, and aliphatic and aromatic compounds derived from humic substances.
3. Fouling appeared to have developed through different stages as reflected in the differences in composition and structure of the fouling layer depending on its thickness. In particular, it consisted of an initial thin fouling layer of an amorphous matrix with embedded particulate matter. The amorphous matrix comprised organic–Al–P complexes and the particulate matter was mostly aluminium silicates. Subsequently, as the fouling layer reached a thickness of about 5–7  $\mu\text{m}$ , a secondary amorphous material, which is suggested to be proteinaceous in nature and could include extracellular polymeric substances such as polysaccharides, started to deposit on top of the existing fouling layer. This secondary amorphous material did not seem to contain any particulate matter or any inorganic elements within it, but acted as a substrate upon which aluminium silicate crystals grew exclusively in the absence of other foulants including NOM.

A key difference between the approach adopted in the current study and those applied in previous autopsy studies is that the current study investigates not only the top surface but also the cross-section of the fouled membrane. As can be seen in this study, the information obtained from the cross-section investigation provides insights into deposition kinetics, which are important for the development of a more complete understanding of the fouling mechanisms. Such information would not be readily available from the traditional approach of analysing the top surface. In this study, the absence of NOM and inorganic particulate matter in the secondary fouling layer and the exclusive growth of aluminium silicates on top of this layer are particularly interesting. Work is already underway to identify the nature of this layer, which, as suggested, could include extracellular polymeric substances. This information, together with the identification and isolation of bacterial strains responsible for the production of these extracellular polymeric substances, may have implications in the development of anti-fouling strategies aimed at preventing the deposition of NOM and particulate matter on RO membranes.

#### Acknowledgment

This work was funded in part by a grant from CSIRO National Research Flagships Program. The authors would like to thank Anita Hill for helpful discussions, Buu Dao and James Mardel for the FTIR analyses, and Yesim Gozukara for the ICP-AES work.

#### REFERENCES

- Belfort, G., Guter, G.A., 1972. An experimental study of electro-dialysis hydrodynamics. *Desalination* 10, 221–262.
- Boerlage, S.F.E., Kennedy, M.D., Witkamp, G.J., van der Hoek, J.P., Schippers, J.C., 1999. BaSO<sub>4</sub> solubility prediction in reverse osmosis systems. *J. Membr. Sci.* 159, 47–59.
- Butt, F.H., Rahman, F., Baduruthamal, U., 1995. Identification of scale deposits through membrane autopsy. *Desalination* 101, 219–230.
- Butt, F.H., Rahman, F., Baduruthamal, U., 1997. Characterization of foulants by autopsy of RO desalination membranes. *Desalination* 114, 51–64.
- Dalvi, A.G.I., Al-Rasheed, R., Javeed, M.A., 2000. Studies on organic foulants in the seawater feed of reverse osmosis plants of SWCC. In: *Proceedings of the Conference on Membranes in Drinking and Industrial Water Production*, vol. 2, Paris, France. Desalination Publications, L'Aquila, Italy, pp. 459–474.
- Gabelich, C.J., Yun, T.I., Coffey, B.M., Suffet, I.H., 2002. Effects of aluminium sulfate and ferric chloride coagulant residuals on polyamide membrane performance. *Desalination* 150, 15–30.
- Gabelich, C.J., Chen, W.R., Yun, T.I., Coffey, B.M., Suffet, I.H., 2005. The role of dissolved aluminum in silica chemistry for membrane processes. *Desalination* 180, 307–319.
- Gimmelshtein, M., Semiat, R., 2005. Investigation of flow next to membrane walls. *J. Membr. Sci.* 264, 137–150.
- Goodhew, P.J., Humphreys, F.J., 1992. *Electron Microscopy and Analysis*, second ed. Taylor & Francis Ltd., London.



- Gwona, E.M., Yu, M.J., Oh, H.K., Ylee, Y.H., 2003. Fouling characteristics of NF and RO operated for removal of dissolved matter from groundwater. *Water Res.* 37, 2989–2997.
- Hartley, P.G., McArthur, S.L., McLean, K.M., Griesser, H.J., 2002. Physicochemical properties of polysaccharide coatings based on grafted multilayer assemblies. *Langmuir* 18, 2483–2494.
- Herzberg, M., Elimelech, M., 2007. Biofouling of reverse osmosis membranes: role of biofilm-enhanced osmotic pressure. *J. Membr. Sci.* 295, 11–20.
- Hoek, E.M.V., Elimelech, M., 2003. Cake-enhanced concentration polarization: a new fouling mechanism for salt-rejecting membranes. *Environ. Sci. Technol.* 37, 5581–5588.
- Ivnitskya, H., Katza, I., Minzc, D., Shimonid, E., Chene, Y., Tarchitzkye, J., Semiatb, R., Dosoretza, C.G., 2005. Characterization of membrane biofouling in nanofiltration processes of wastewater treatment. *Desalination* 185, 255–268.
- Kumar, M., Adham, S., Pearce, W.R., 2006. Investigation of seawater reverse osmosis fouling and its relationship to pretreatment type. *Environ. Sci. Technol.* 40, 2037–2044.
- Lee, S., Cho, J., Elimelech, M., 2005. Combined influence of natural organic matter (NOM) and colloidal particles on nanofiltration membrane fouling. *J. Membr. Sci.* 262, 27–41.
- Li, Q., Elimelech, M., 2004. Organic fouling and chemical cleaning of nanofiltration membranes: measurements and mechanisms. *Environ. Sci. Technol.* 38, 4683–4693.
- Li, Q., Elimelech, M., 2006. Synergistic effects in combined fouling of a loose nanofiltration membrane by colloidal materials and natural organic matter. *J. Membr. Sci.* 278, 72–82.
- Riggle, J., von Wandruszka, R., 2005. Binding of inorganic phosphate to dissolved metal humates. *Talanta* 66, 372–375.
- Sahachaiyunta, P., Koo, T., Sheikholeslami, R., 2002. Effect of several inorganic species on silica fouling in RO membranes. *Desalination* 144, 373–378.
- Speth, T.F., Summers, R.S., Gusses, A.M., 1998. Nanofiltration foulants from a treated surface water. *Environ. Sci. Technol.* 32, 3612–3617.
- Speth, T.F., Gusses, A.M., Summers, R.S., 2000. Evaluation of nanofiltration pretreatments for flux loss control. *Desalination* 130, 31–44.
- Tay, K.G., Song, L., 2005. A more effective method for fouling characterization in a full-scale reverse osmosis process. *Desalination* 177, 95–107.
- Vrouwenvelder, J.S., van der Kooij, D., 2002. Diagnosis of fouling problems of NF and RO membrane installations by a quick scan. *Desalination* 153, 121–124.
- Yiantsios, S.G., Sioutopoulos, D., Karabelas, A.J., 2005. Colloidal fouling of RO membranes: an overview of key issues and efforts to develop improved prediction techniques. *Desalination* 183, 257–272.